

# Identification and Bimodal Speed Control of Ultrasonic Motors Using Input-Output Recurrent Neural Networks<sup>1)</sup>

XU Xu<sup>1</sup> LIANG Yan-Chun<sup>2</sup> SHI Xiao-Hu<sup>2</sup> LIU Shu-Fen<sup>2</sup>

<sup>1</sup>(College of Mathematics Science, Jilin University, Changchun 130012)

<sup>2</sup>(College of Computer Science and Technology, Jilin University, Key Laboratory of Symbol Computation and Knowledge Engineering of the Ministry of Education, Changchun 130012)

(E-mail: xuxu567@mail.jl.cn)

**Abstract** A newly developed input-output recurrent neural network (IORNN) identifier of USM is constructed. A bimodal neural network controller is designed where both the driving frequency and amplitude of the applied voltage are used as control inputs. The dynamic recurrent back-propagation algorithm of the identifier and controller are developed. Numerical results show that the proposed IORNN identifier can approximate the nonlinear input-output mappings of the ultrasonic motor quite well. Good effectiveness of the proposed bimodal IORNN controller is also obtained for some different kinds of reference speeds.

**Key words** Ultrasonic motors, neural network, bimodal controller

## 1 Introduction

Ultrasonic motor (USM) is a newly developed motor which has some excellent performances and useful features and can be widely applied to MEMS, robot, medical instrument, aeronautics, and some others<sup>[1,2]</sup>. The operational characteristics of the USM are affected by many factors. Strongnonlinearity characteristics could be caused by increase of temperature, changes of load, driving frequency and voltage, and many other factors<sup>[3,4]</sup>. Therefore, it is difficult to perform effective control to the USM using traditional control methods based on mathematical models of systems. Recently artificial intelligent methods<sup>[5,6]</sup> based on neural networks have become main approaches to USM control. In most cases the driving frequency is taken as a single control variable<sup>[4]</sup>. The existing neural-network-based methods for USM control have some shortcomings, such as complex network structures, slow convergent speeds and low convergent precision besides the limitation of single control variable. It is difficult to obtain the accurate control input for the USM. When the traditional neural-network-based-method with a single control variable for the USM is adopted, the fluctuation of speed is large for steady state and the convergent speeds are slow.

In this paper, a newly developed bimodal speed control scheme of USM using neural network is designed. In the proposed control scheme both amplitude and driving frequency of the applied voltage can be adjusted simultaneously. By adjusting the amplitude of the applied voltage on line, the speed error caused by inaccurate driving frequency can be compensated. A novel input-output recurrent neural network (IORNN) structure is proposed, and the identifier and the controller of USM with the IORNN structure are constructed. The dynamic recurrent back-propagation algorithm for training the identifier and controller is developed. Numerical results show that the proposed IORNN identifier can approximate the nonlinear input-output mapping of the USM quite well. Good control effectiveness can

1) Supported by National Natural Science Foundation (19872027) and Ministry of Science and Technology of P. R. China

Received June 24, 2002; in revised form November 13, 2002

收稿日期 2002-06-24; 收修改稿日期 2002-11-13

be obtained for various reference speeds. The control precision and the time of convergence using the proposed method are obviously better than those using existing methods.

## 2 Neural network identifier(NNI)

A novel input-output recurrent network (IORNN) identifier of USM presented in this paper is shown in Fig. 1. In the figure, the notation  $\square$  represents the context neuron with self-recurrent gain  $\lambda$  ( $0 \leq \lambda < 1$ ),  $\circ$  the hyperbolic tangential neuron,  $\bullet$  the linear neuron,  $C \in R^{N \times H}$  the weight matrix associated with the context and hidden neurons,  $D \in R^H$  the weight vector associated with the hidden and output neurons,  $N$  the number of the input nodes, and  $H$  the number of the neurons in the hidden layer. The outputs of the input nodes are exerted directly on the context neurons. For convenience, we denote the outputs of input nodes as  $I = \{I_i\}_{i=1}^N$ , the outputs of the context neurons as  $z = \{z_i\}_{i=1}^N$ , and the outputs of the hidden neurons as  $x = \{x_j\}_{j=1}^H$ . The output of the context neuron is:

$$\begin{cases} z_i(k) = I_i(k) + \lambda z_i(k-1) = \\ I_i(k) + \lambda I_i(k-1) + \lambda^2 I_i(k-2) + \cdots + \lambda^{k-1} I_i(1) = \sum_{l=1}^k \lambda^{k-l} I_i(l) \\ z_i(0) = 0, (i = 1, 2, \dots, N) \end{cases}$$

The block diagram of the identification model proposed in this paper is shown in Fig. 2. In the figure, USM denotes the ultrasonic motor, NNI the neural network identifier,  $u(k)$  and  $\omega(k)$  the amplitude of the applied voltage and driving frequency, respectively,  $y(k)$  the actual speed of the USM,  $y_I(k)$  the output of the NNI,  $z^{-1}$  the time delay of the speed of the USM.  $e_I(k) = y(k) - y_I(k)$  the error between the actual speed of the USM and the output of the NNI.

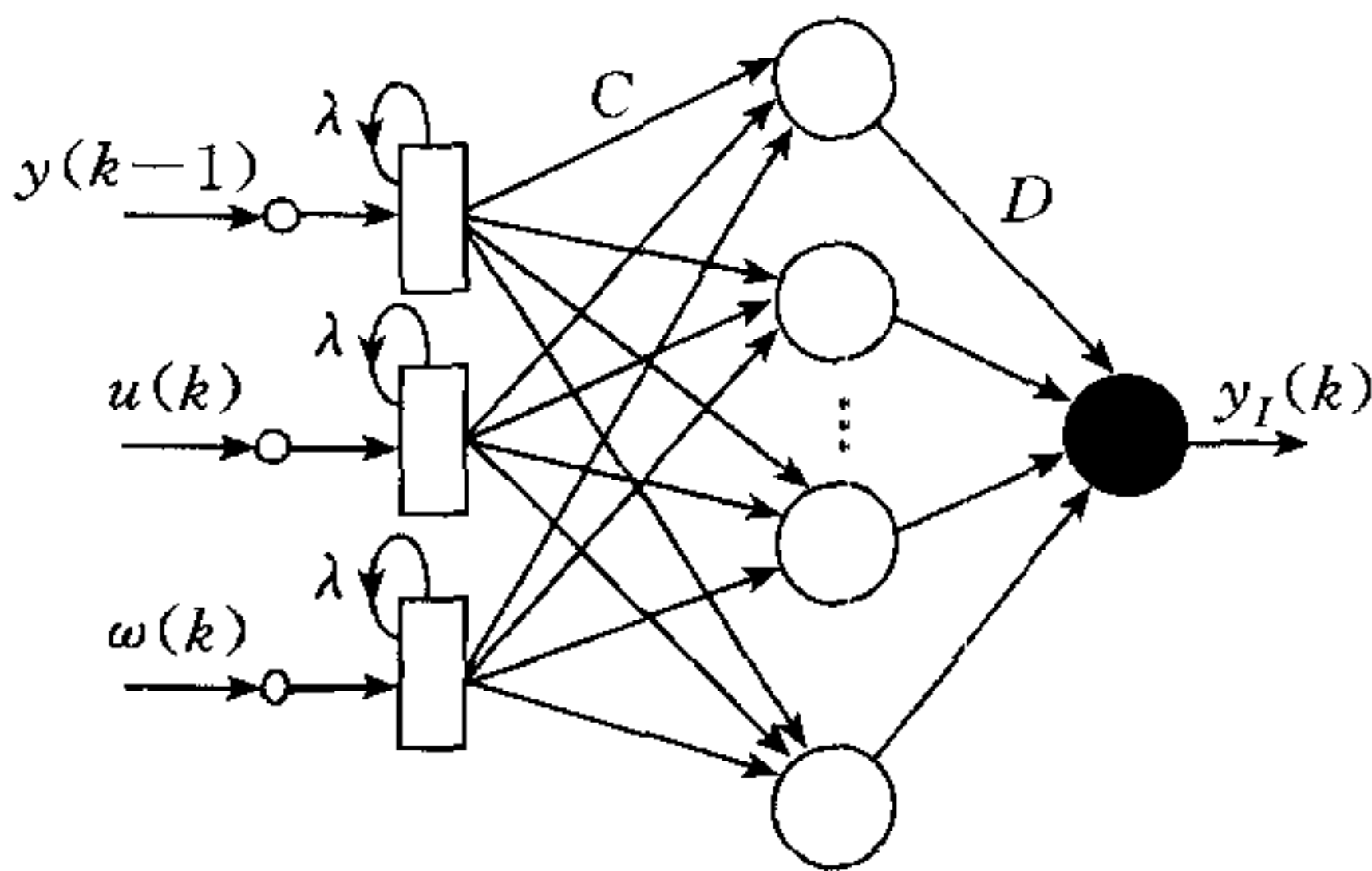


Fig. 1 Architecture of neural network identifier(NNI)

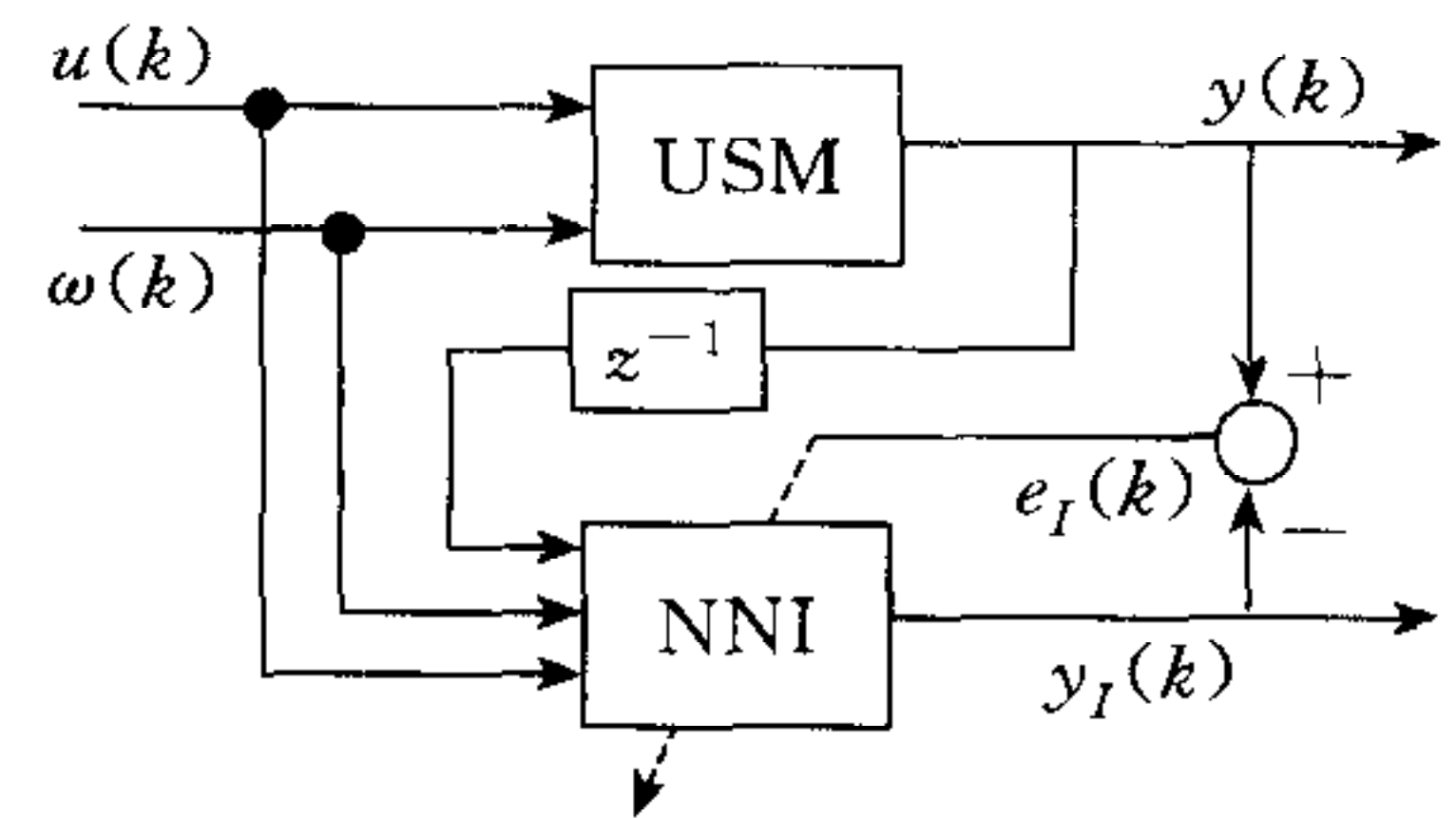


Fig. 2 Block diagram of identification

The Dynamic training algorithm of the NNI is discussed as follow. For convenience, in this section the values of subscripts  $i$  and  $j$  are taken as  $i = 1, 2, \dots, N$ ;  $j = 1, 2, \dots, H$ .

The outputs of the neurons in the hidden and output layers of the NNI are

$$y_I(k) = \sum_{j=1}^H (D_j(k) x_j(k)), \quad x_j(k) = f\left(\sum_{i=1}^N C_{ij}(k) z_i(k)\right) = f(S_j(k))$$

where  $S_j(k) = \sum_{i=1}^N C_{ij}(k) z_i(k)$ ,  $f(x) = \frac{1 - e^{-x}}{1 + e^{-x}}$  is the hyperbolic tangential function. The

error function is defined as  $E_I(k) = \frac{1}{2} e_I^2(k)$ . Let  $\mu_d(k)$  be the learning rate for weights  $D$  and  $\mu_c(k)$  be the learning rate for weights  $C$ . The modification of the weights associated with the hidden and output layers is

$$\Delta D_j = -\mu_d(k) \frac{\partial E_I(k)}{\partial D_j} = -\mu_d(k) e_I(k) \frac{\partial e_I(k)}{\partial D_j} = \mu_d(k) e_I(k) \frac{\partial y_I(k)}{\partial D_j}$$



$$\Delta C_{ij} = -\mu_c(k) \frac{\partial E_1(k)}{\partial C_{ij}} = \mu_c(k) e_1(k) \frac{\partial y_1(k)}{\partial x_j(k)} \frac{\partial x_j(k)}{\partial C_{ij}} = \mu_c(k) e_1(k) D_j \frac{\partial x_j(k)}{\partial C_{ij}}$$

Denote  $f'_j(k) = \frac{\partial f(S_j(k))}{\partial S_j(k)}$ . Supposing that the sampling interval is small enough and noticing that the derivative of the hyperbolic tangential function is continuous, we may think that  $f'_j(k) \approx f'_j(k-1)$ . Then we have

$$\begin{aligned} \frac{\partial x_j(k)}{\partial C_{ij}} &= f'_j(k) z_i(k) = f'_j(k) I_i(k) + \lambda \frac{f'_j(k)}{f'_j(k-1)} \frac{\partial x_j(k-1)}{\partial C_{ij}} \approx \\ & f'_j(k) I_i(k) + \lambda \frac{\partial x_j(k-1)}{\partial C_{ij}} \end{aligned}$$

According to the back-propagation algorithm,  $D_j(k)$  and  $C_{ij}(k)$  of the NNI are

$$D_j(k) = D_j(k-1) + \Delta D_j(k), \quad C_{ij}(k) = C_{ij}(k-1) + \Delta C_{ij}(k)$$

During the computation the control variables  $u(k)$  and  $\omega(k)$  are inputted into the USM and NNI simultaneously to calculate the error between the actual speed of the USM and the output of the NNI. The modification of the weights is performed using the dynamic training algorithm described in this section.

### 3 Speed control of USM

The bimodal speed control system proposed in this paper is shown in Fig. 3. In the figure, NNC represents the neural network controller, USM the ultrasonic motor, NNI the neural network identifier,  $y_m(k)$  the speed control value,  $y(k)$  the actual speed,  $e_c = y_m(k) - y(k)$  the error between the actual and control speeds, and  $y_1(k)$  the output of the identified model. The NNC shown in Fig. 4 also adopts IORNN structure. To simplify the structure of the neural network we use only two inputs  $y_m(k)$  and  $y(k-1)$ .  $A \in R^{N^c \times H^c}$  is the weight matrix associated with the context and hidden neurons,  $B \in R^{H^c \times L}$  the weight matrix associated with the hidden and output neurons,  $N^c$  the number of the input nodes which is chosen as 2 in this paper,  $H^c$  the number of the neurons in the hidden layer,  $L$  the number of the output neurons which is chosen as 2 in this paper,  $u$  and  $\omega$  the amplitude and frequency of the driving voltage, respectively. Denote the outputs of the input nodes in the NNC as  $I^c(k) = \{I_i^c(k)\}_{i=1}^{N^c}$ , the outputs of the context neurons as  $z^c(k) = \{z_i^c(k)\}_{i=1}^{N^c}$ , and the outputs of the hidden neurons as  $x^c = \{x_i^c(k)\}_{i=1}^{H^c}$ .

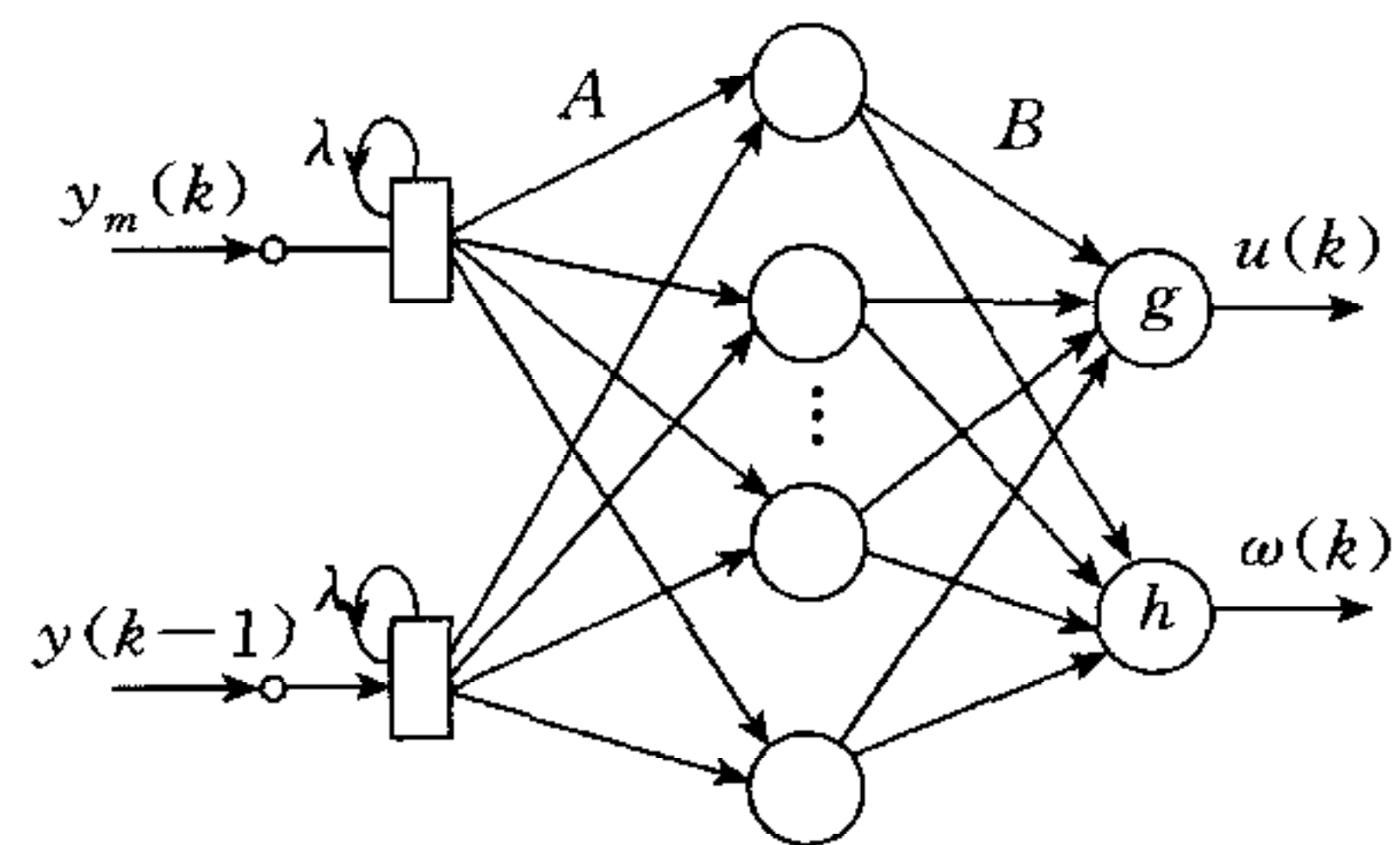
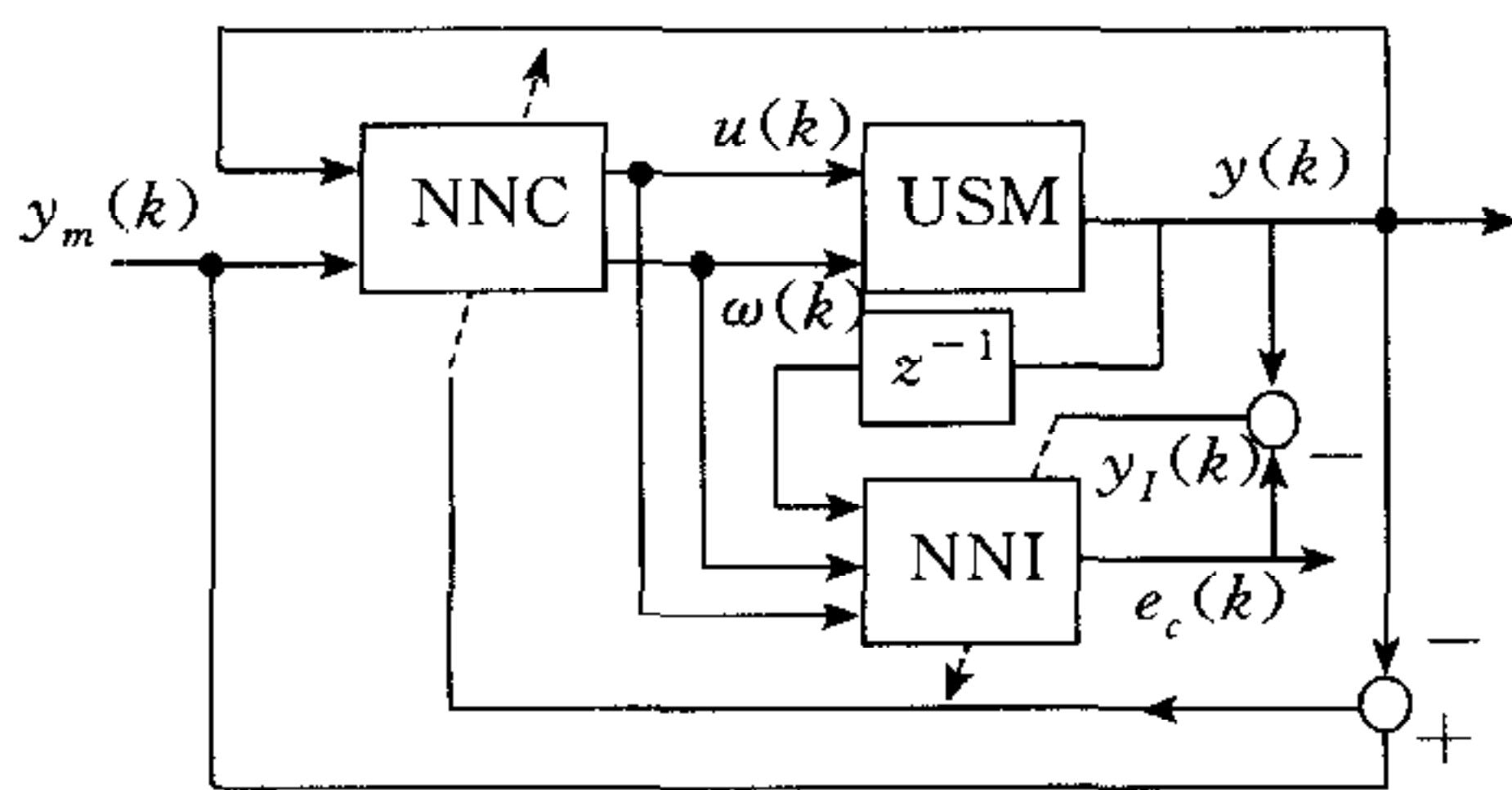


Fig. 3 Block diagram of speed control system Fig. 4 Architecture of neural network controller(NNC)

Considering the characteristics of the driving voltage, we take the activation functions of the neurons in the output of the NNC as

$$g(x) = \alpha \frac{1 - e^{-x}}{1 + e^{-x}} + u^*, \quad h(x) = \frac{1 - e^{-x}}{1 + e^{-x}} + \omega^*$$

where  $g(x)$  and  $h(x)$  are the activation functions associated with the outputs  $u$  and  $\omega$ , respectively,  $u^*$  and  $\omega^*$  the allowed amplitude and frequency of the driving voltage, respectively, and  $\alpha > 0$  an adjustable parameter. The activation function for the neurons in the

hidden layer is still taken as the hyperbolic tangential function.

In this section the subscripts  $i, j$  and  $l$  are taken as  $i=1, 2, \dots, N^c$ ;  $j=1, 2, \dots, H^c$ ;  $l=1, 2$ . The derivatives of the speed of USM with respect to the control inputs are needed in order to modify the weights of the NNC, which can be calculated approximately by using the NNI.

Noticing that  $I_2(k) = u(k)$ , we have  $\frac{\partial z_1(k)}{\partial u(k)} = 0$ ,  $\frac{\partial z_2(k)}{\partial u(k)} = 1$ ,  $\frac{\partial z_3(k)}{\partial u(k)} = 0$ , so

$$\frac{\partial y(k)}{\partial u(k)} \approx \frac{\partial y_I(k)}{\partial u(k)} = \sum_{j=1}^H \frac{\partial y_I(k)}{\partial x_j(k)} \frac{\partial x_j(k)}{\partial u(k)} = \sum_{j=1}^H D_j(k) f'_j(k) C_{2j}(k)$$

In a similar way, we have,  $\frac{\partial y(k)}{\partial \omega(k)} \approx \frac{\partial y_I(k)}{\partial \omega(k)} = \sum_{j=1}^H D_j(k) f'_j(k) C_{3j}(k)$ . The outputs of the neurons of the hidden and output layers in the NNC can be rewritten respectively as:

$$x_j^c(k) = f\left(\sum_i^{N^c} (A_{ij}(k) z_i^c(k))\right), \quad u(k) = g\left(\sum_{j=1}^{H^c} (B_{j1}(k) x_j^c(k))\right),$$

$$\omega(k) = h\left(\sum_{j=1}^{H^c} (B_{j2}(k) x_j^c(k))\right).$$

Let  $\mu_B(k)$  be the learning rate for weights  $B$ , and  $\mu_A(k)$  be the learning rate for weights  $A$ . The modification of the weights associated with the hidden and the output layers is

$$\Delta B_{jl}(k) = -\mu_B(k) \frac{\partial E_c(k)}{\partial B_{jl}} \approx \mu_B(k) e_c(k) \left( \frac{\partial y_I(k)}{\partial u(k)} \frac{\partial u(k)}{\partial B_{jl}} + \frac{\partial y_I(k)}{\partial \omega(k)} \frac{\partial \omega(k)}{\partial B_{jl}} \right) =$$

$$\mu_B(k) e_c(k) \left[ \frac{\partial y_I(k)}{\partial u(k)} g'(k) + \frac{\partial y_I(k)}{\partial \omega(k)} h'(k) \right] x_j^c(k)$$

where  $E_c(k) = \frac{1}{2} e_c^2(k)$ ,  $\frac{\partial u(k)}{\partial B_{j2}} = 0$ ,  $\frac{\partial \omega(k)}{\partial B_{j1}} = 0$ .

The modification of the weights associated with the context and the hidden neurons is

$$\Delta A_{ij}(k) = -\mu_A(k) \frac{\partial E_c(k)}{\partial A_{ij}} \approx \mu_A(k) e(k) \left( \frac{\partial y_I(k)}{\partial u(k)} \frac{\partial u(k)}{\partial A_{ij}} + \frac{\partial y_I(k)}{\partial \omega(k)} \frac{\partial \omega(k)}{\partial A_{ij}} \right) =$$

$$\mu_A(k) e(k) \left[ \frac{\partial y_I(k)}{\partial u(k)} g'(k) B_{j1}(k) + \frac{\partial y_I(k)}{\partial \omega(k)} h'(k) B_{j2}(k) \right] \frac{\partial x_j^c(k)}{\partial A_{ij}}$$

here,  $\frac{\partial x_j^c(k)}{\partial A_{ij}} = f'_{c_j}(k) z_i^c(k) = f'_{c_j}(k) I_i^c(k) + \lambda \frac{f'_{c_j}(k)}{f'_{c_j}(k-1)} \frac{\partial x_j^c(k-1)}{\partial A_{ij}}$

$$\approx f'_{c_j}(k) I_i^c(k) + \lambda \frac{\partial x_j^c(k-1)}{\partial A_{ij}}$$

According to the back-propagation algorithm update rules of the weights,  $B_{jl}(k)$  and  $A_{ij}(k)$  of the NNC are  $B_{jl}(k) = B_{jl}(k-1) + \Delta B_{jl}(k)$ , and  $A_{ij}(k) = A_{ij}(k-1) + \Delta A_{ij}(k)$ , respectively.

#### 4 Numerical simulation results and discussions

Numerical simulations are performed using the proposed method for the speed control of a longitudinal oscillation USM<sup>[7, 8]</sup> shown in Fig. 5. Some parameters on the USM model are taken as: driving frequency 27.8KHz, amplitude of driving voltage 300V, allowed output moment 2.5N·cm, rotation speed 3.8m/s. The adjustable parameter  $\alpha$  is taken as 5.0 and the gain factor  $\lambda$  in the NNI and NNC are taken as 0.65.

Fig. 6 shows the output curves of the USM and the NNI for the same input near the allowed frequency and amplitude of the driving voltage. In addition, an external moment of 1N·cm is exerted on the USM during the operation interval between the 8th second and 9th second. In the figure, the solid line represents the simulated experimental curve obtained using the USM model in [3] and the dotted line represents the identified curve



obtained using the proposed neural network model in this paper. It can be seen that the results obtained from this paper are basically identical to those obtained from the simulated experiments.

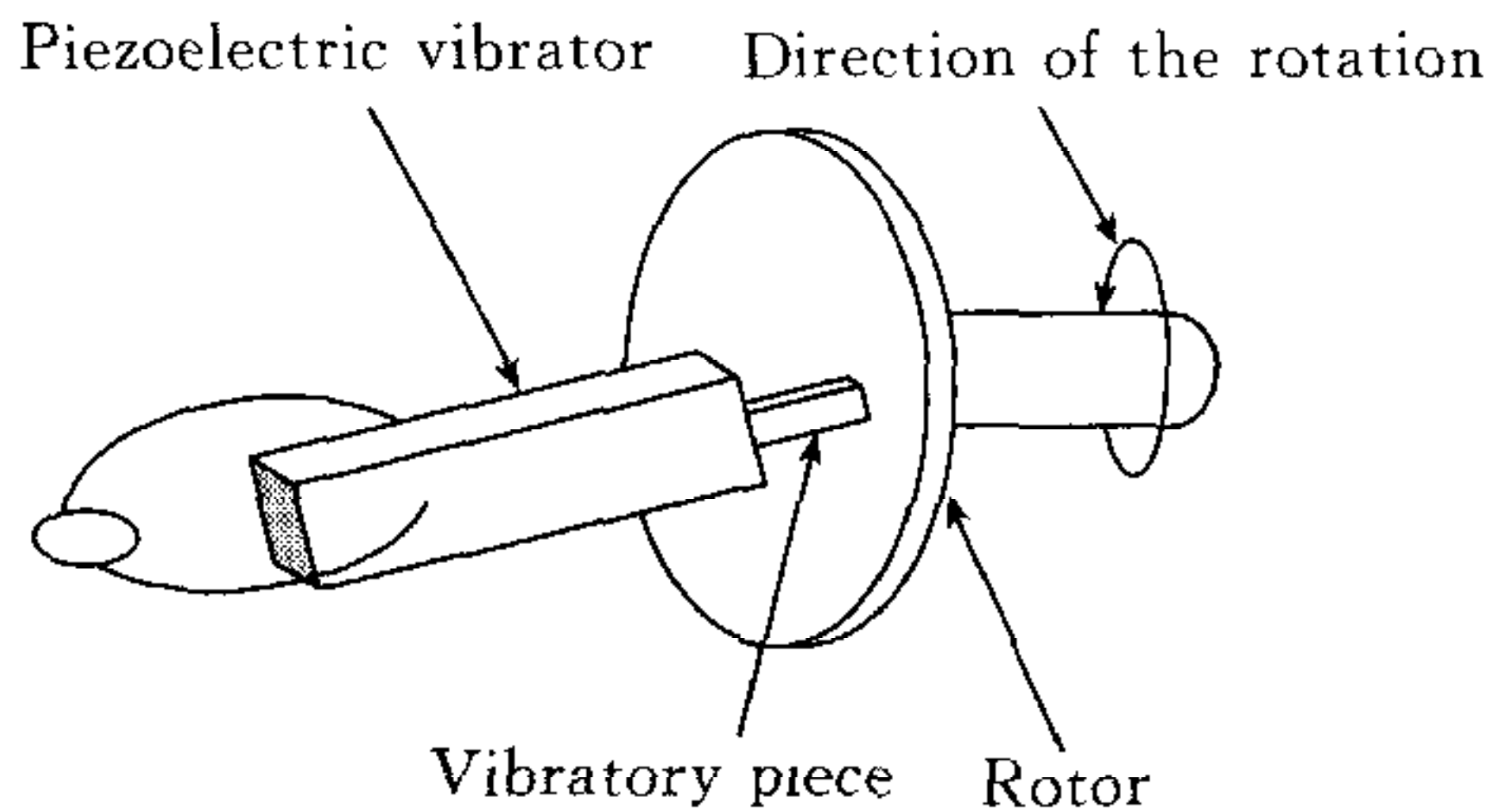


Fig. 5 Schematic diagram of the motor

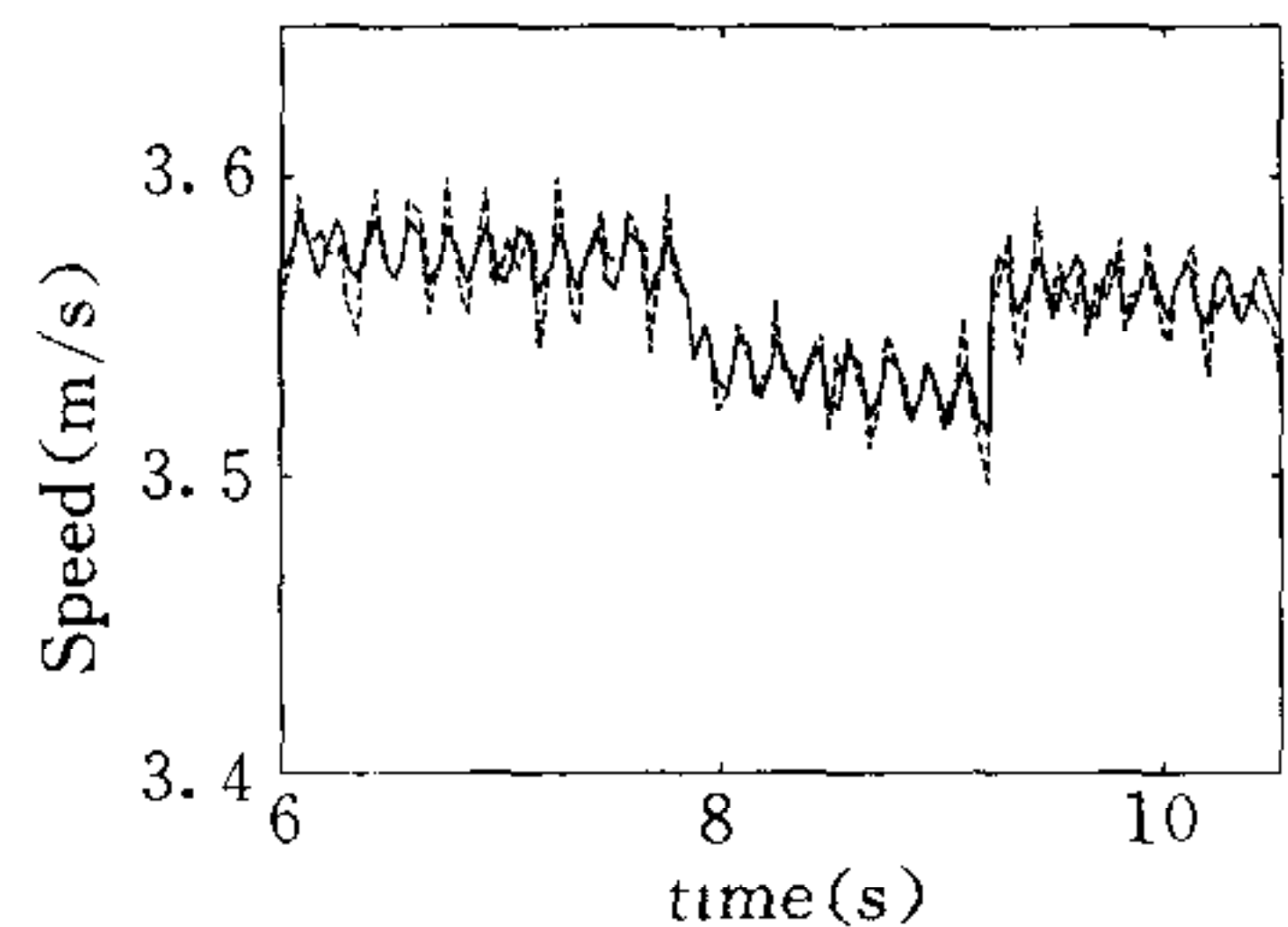


Fig. 6 Comparison of experimental and identified speed curves

Fig. 7 shows the comparison of speed control curves of USM using the conventional neural network control method and the method proposed in this paper when the control speed is taken as 3.6m/s and the external moment is taken as 1N • cm. Fig. 8 shows the cases of the fluctuation with two different control schemes. In the two figures, the dotted line represents the speed control curve based on the method presented in [4] and the solid line represents the speed curve using the method proposed in this paper. The fluctuation is defined as  $\zeta = (V_{max} - V_{min}) / V_{aver} \times 100\%$ , where  $V_{max}$ ,  $V_{min}$  and  $V_{aver}$  represent the maximum, minimum and average values of the speed, respectively. From the figures it can be seen that the fluctuation is large when the method in [4] is employed, the average fluctuation reaches 5.7%, whereas, it is just 1.4% when the method of this paper is used. The comparison shows that the control precision can be increased by around 3 times when the proposed method is employed.

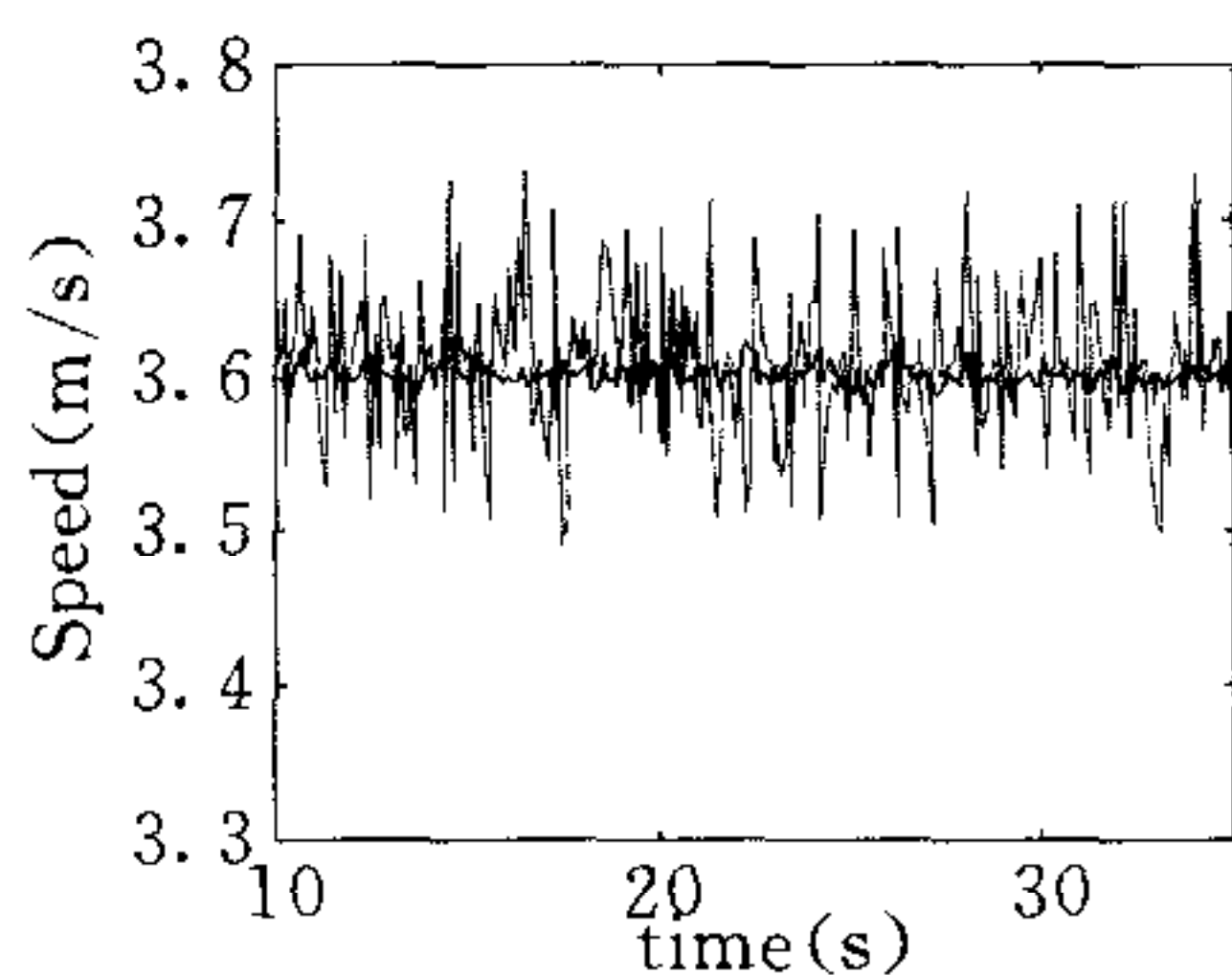


Fig. 7 Comparison of speed control curves using different control schemes

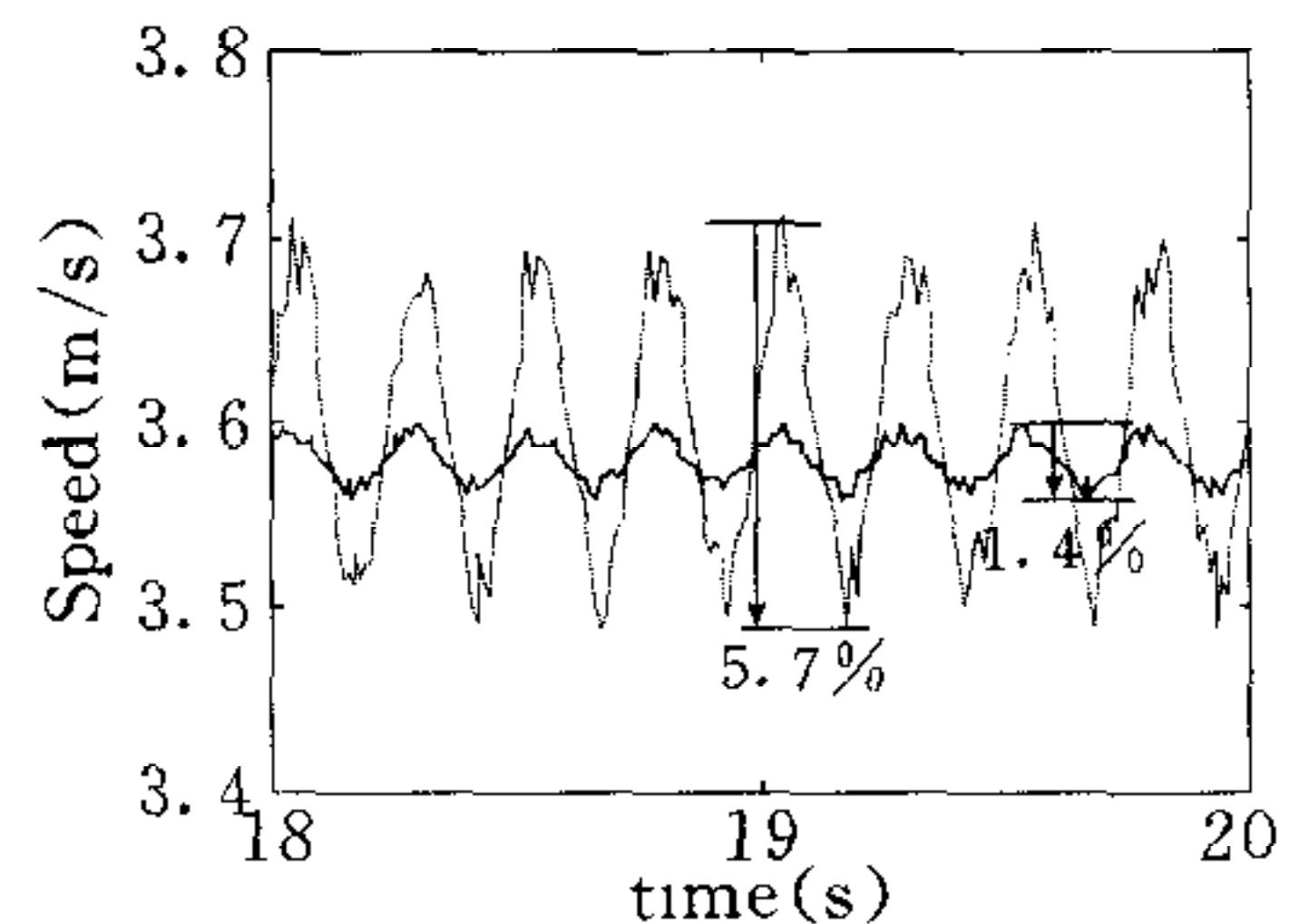


Fig. 8 Comparison of speed fluctuation using different schemes

Fig. 9 shows the speed control curves, where the reference speeds vary as step type at the beginning and as sinusoidal type afterward, and the dotted line represents the speed control curve based on the method proposed in this paper and the solid line represents the reference speed curve. From the figure it can be seen that this method possesses good control precision.

Fig. 10 shows the comparison of the average errors using the conventional neural network control method<sup>[4]</sup> and the method proposed in this paper. In the figure, the dotted line represents the average error curve obtained using the method in [4], the solid line represents the results obtained using the method proposed in this paper. From the figure it can be seen that the time of convergence using the proposed method is about 6 seconds, which is much shorter than 17 seconds, the time of convergence using the existing meth-

od<sup>[4]</sup>. From the comparison it can be seen that the proposed method is superior to the existing method in the speed of convergence.

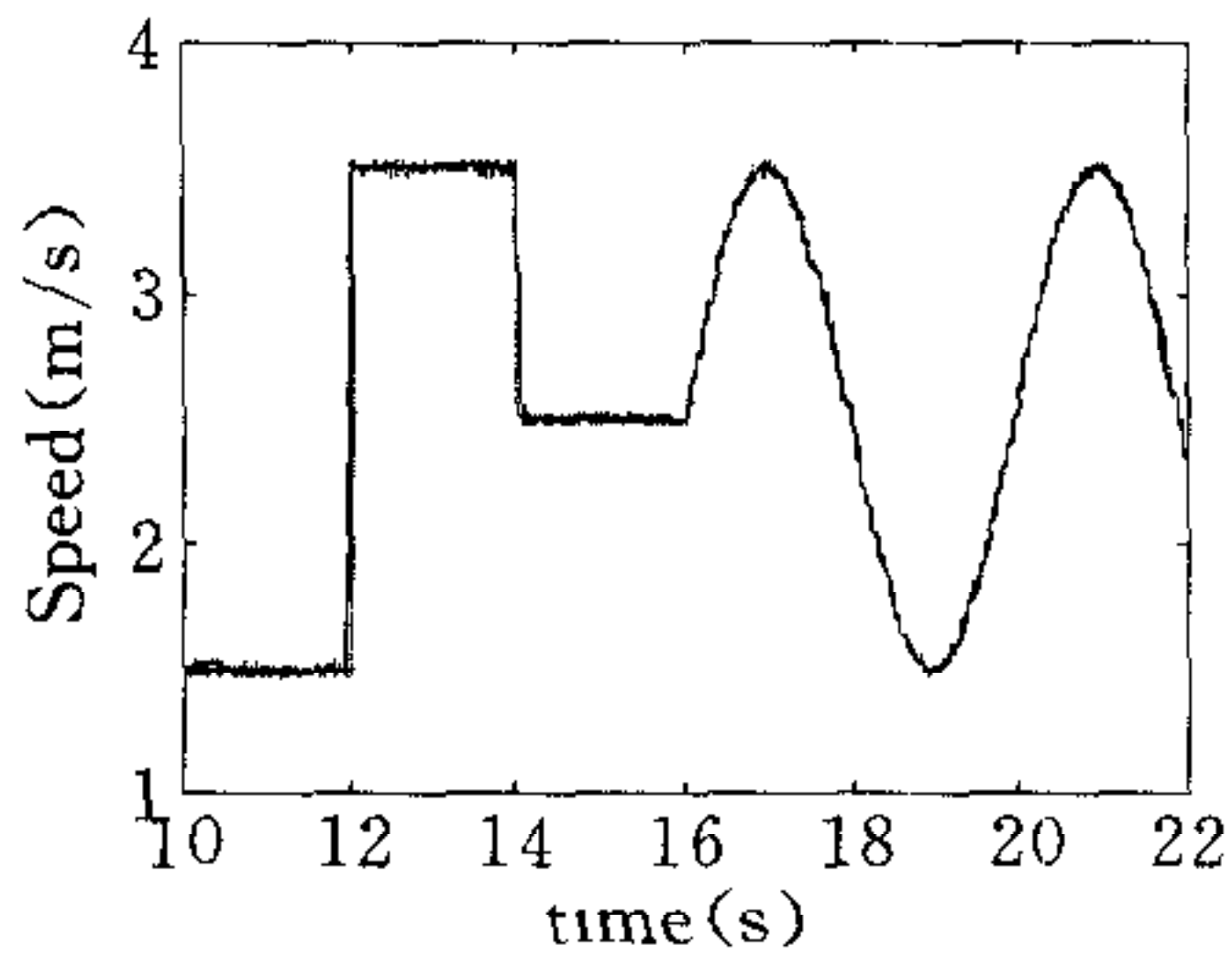


Fig. 9 Speed control curves with varied reference speeds

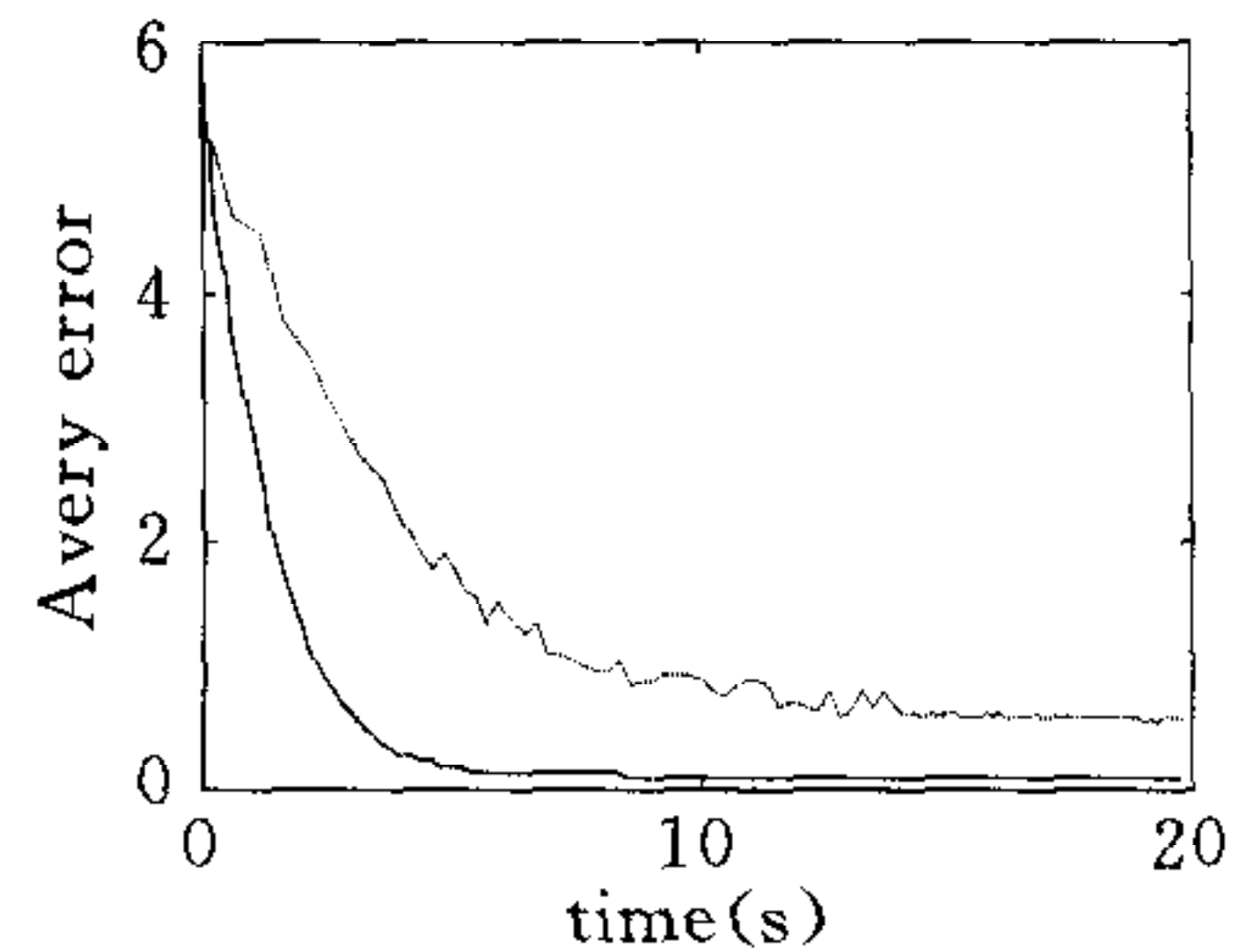


Fig. 10 Comparison of average errors using different neural network structures

## 5 Conclusions

An identification and speed control model for ultrasonic motors is presented based on neural networks. The input-output relation of the USM is identified dynamically using the proposed model. A bimodal controller is designed using the frequency and amplitude of the driving voltage as control inputs. The dynamic recurrent back-propagation algorithm of the identifier and controller are developed. Numerical simulations of a longitudinal oscillation USM show that the proposed model can approximate the nonlinear input-output mapping of the USM quite well. The effect and applicability of the proposed model are examined using different kinds of speeds with constant, step, and sinusoidal types. The method would also be useful for controlling and identifying different types of speeds of the piezoelectric motor or USM besides the longitudinal oscillation USM.

## References

- 1 Sashida T, Kenjo T. An Introduction to Ultrasonic Motors. Oxford: Clarendon Press, 1993
- 2 Ueha S, Tomikawa T. Piezoelectric Motors: Theory and Application. Oxford: Science Publications, 1993
- 3 Xu X, Liang Y C, Shi X H. Analysis of frequency-temperature characteristics of ultrasonic motors. *Journal of Jilin University (Science Edition)*, 2002, **40**(2): 109~113
- 4 Senjyu T, Miyazato H, Yokoda S, Uezato K. Speed control of ultrasonic motors using neural network. *IEEE Transactions on Power Electronics*, 1998, **13**(3): 381~387
- 5 Hu S S, Zhou C, Hu W L. Model-following robust adaptive control based on neural networks. *Acta Automatica Sinica*, 2000, **26**(5): 623~629
- 6 Liang Y C, Lin W Z, Lee H P, Lim S P, Lee K H, Feng D P. A neural-network-based method of model reduction for dynamic simulation of MEMS. *Journal of Micromechanics and Microengineering*, 2001, **11**(3): 226~233
- 7 Xu X, Liang Y C, Shi X H. Mechanical modeling of a longitudinally vibration ultrasonic motor. *Acta Acustica*, 2003, **28**(3): 223~228
- 8 Sashida T. Trial construction and operation of an ultrasonic vibration driven motor; Theoretical and experimental investigation of its performances. *Oyo Buturi*, 1982, **51**(6): 713~720 (in Japanese)

**XU Xu** Received his master degree and Ph. D. degree from Jilin University in 1997 and 2003, respectively. His research interests include the ultrasonic motor and intelligence control.

**LIANG Yan-Chun** Received his master and Ph. D. degrees from Jilin University in 1982 and 1997, respectively. Currently he is a professor in College of Computer Science and Technology of Jilin University. His research interests include computational intelligence, modeling and the model reduction of MEMS and intelligent control.

**SHI Xiao-Hu** Received his master degree from Jilin University in 2002. Currently he is a Ph. D. candidate in College of Computer Science and Technology of Jilin University. His research interests include applications of computer and artificial neural networks.

**LIU Shu-Fen** Graduated from Electronics Department of Jilin University in 1975. Currently she is a professor in College of Computer Science and Technology of Jilin University. Her research interests include



computer networks and security technique.

## 基于输入输出回归神经网络的超声马达辨识和速度控制

徐 旭<sup>1</sup> 梁艳春<sup>2</sup> 时小虎<sup>2</sup> 刘淑芬<sup>2</sup>

<sup>1</sup>(吉林大学数学学院 长春 130012)

<sup>2</sup>(吉林大学计算机科学与技术学院, 国家教育部符号计算与知识工程重点实验室 长春 130012)

(E-mail: xuxu567@mail.jl.cn)

**摘 要** 建立了一个新的输入-输出反馈神经网络结构用于超声马达速度辨识. 给出了以驱动电压的幅值和驱动频率为控制量的双模式速度控制器, 推导了辨识器和控制器的动态递归反传算法. 数值模拟结果表明, 辨识器能比较精确地描述马达的输入-输出关系, 双模式神经网络控制器对多种形式的参考速度, 都有很好的控制效果.

**关键词** 超声马达, 神经网络, 双模式控制器

**中图分类号** TP11

---

### A Correction Note (更正)

The title of the special issue in ACTA AUTOMATICA SINICA, Vol. 29, No. 3, should be "Special Issue on Visual Surveillance of Dynamic Scenes". Some of the copies have a typographical error on the title.

(本刊 2003 年 29 卷第 3 期(部分)封面专刊标题应为"Special Issue on Visual Surveillance of Dynamic Scenes", 特此更正. 并对由此给读者带来的不便表示歉意.)"